The University of
Nottingham

UNITED KINGDOM · CHINA · MALAYSIA

Abdullah, Zuraidah and Bayraktutan, Ulvi (2016) Suppression of PKC-α attenuates TNF-α-evoked cerebral barrier breakdown via regulations of MMP-2 and plasminogen–plasmin system. Biochimica et Biophysica Acta (BBA) - Molecular Basis of Disease, 1862 (7). pp. 1354-1366. ISSN 0006-3002

Access from the University of Nottingham repository:
http://eprints.nottingham.ac.uk/37937/1/Suppression%20of%20PKC-%CE%B1%20attenuates%20TNF-%CE%B1-evoked%20x.pdf

Suppression of PKC-α attenuates TNF-α-evoked cerebral barrier breakdown via regulations of MMP-2 and plasminogen-plasmin system

Zuraidah Abdullah[a] and Ulvi Bayraktutan[a*]

[a] Stroke, Division of Clinical Neuroscience, Clinical Sciences Building, School of Medicine, Hucknall Road, Nottingham, NG5 1PB, UK

*Corresponding author
Dr Ulvi Bayraktutan,
Associate Professor
Stroke, Division of Clinical Neuroscience
Clinical Sciences Building
School of Medicine
The University of Nottingham
Hucknall Road
Nottingham
NG5 1PB
UK

Tel: +44-(115)8231764
Fax: +44-(115)8231767
E-mail: ulvi.bayraktutan@nottingham.ac.uk

Running title

Inhibition of PKC-α negates TNF-α-evoked barrier damage

Abstract

Ischaemic stroke, accompanied by neuroinflammation, impairs blood-brain barrier integrity through a complex mechanism involving both protein kinase C (PKC) and urokinase. Using an *in vitro* model of human blood-brain barrier (BBB) composed of brain microvascular endothelial cells (HBMEC) and astrocytes, this study assessed the putative roles of these elements in BBB damage evoked by enhanced availability of pro-inflammatory cytokine, TNF-α. Treatment of HBMEC with TNF-α significantly increased the mRNA and protein expressions of all plasminogen-plasmin system (PPS) components, namely tissue plasminogen activator, urokinase, urokinase plasminogen activator receptor and plasminogen activator inhibitor-1 and also the activities of urokinase, total PKC and extracellular MMP-2. Inhibition of urokinase by amiloride abated the effects of TNF-α on BBB integrity and MMP-2 activity without affecting that of total PKC. Conversely, pharmacological inhibition of conventional PKC isoforms dramatically suppressed TNF-α-induced overactivation of urokinase. Knockdown of PKC-α gene via specific siRNA in HBMEC suppressed the stimulatory effects of TNF-α on protein expression of all PPS components, MMP-2 activity, DNA fragmentation rates and pro-apoptotic caspase-3/7 activities. Establishment of co-cultures with BMEC transfected with PKC-α siRNA attenuated the disruptive effects of TNF-α on BBB integrity and function. This was partly due to elevations observed in expression of a tight junction protein, claudin-5 and partly to prevention of stress fibre formation. In conclusion, specific inhibition of PKC-α in cerebral conditions associated with exaggerated release of pro-inflammatory cytokines, notably TNF-α may be of considerable therapeutic value and help maintain endothelial cell viability, appropriate cytoskeletal structure and basement membrane.

Keywords:

TNF-α; blood-brain barrier; PKC-α; PPS components; MMP-2; claudin-5; apoptosis; stress fibres.

Abbreviations

Tumour necrosis factor-alpha (TNF-α); protein kinase C-alpha (PKC-α); plasminogen-plasmin system (PPS); blood-brain barrier (BBB); human brain microvascular endothelial cells (HBMEC); sodium fluorescein (NaF); Evan's blue-labelled albumin (EBA); transendothelial electrical resistance (TEER); foetal bovine serum (FBS); phosphate-buffered saline (PBS); Hank's Balanced Salt Solution (HBSS); matrix metalloproteinase (MMP); diphenyleneiodonium (DPI); tight junctions (TJ)

1. Introduction

Blood-brain barrier (BBB) is located between cerebral circulation and the brain and accounts for the selective transition of ions and molecules between the two [1]. The BBB is composed of an endothelial cell lining surrounded by a continuous basement membrane and astrocyte endfeet as well as pericytes and neurons [2-4]. In addition to astrocyte endfeet, tight junctions also determine the overall tightness of BBB. They exist between adjacent endothelial cells and are formed by intricate relationships between claudin-5 and occludin proteins themselves and with the actin cytoskeleton. Taken together, these findings imply that any physical, chemical or humoral pathological stimulus that can alter the structure or function of any of the abovementioned components would undoubtedly alter the permeability of BBB [5, 6].

Neuroinflammation, characterised by an excessive generation of inflammatory cytokines, notably TNF-α, has long been regarded a key phenomenon in breakdown of the BBB after an ischaemic stroke. Recent studies scrutinising the molecular causes of TNF-α-induced BBB damage have proven concurrent inductions of matrix metalloproteinase-2 (MMP-2), a basement membrane degrading enzyme and NADPH oxidase, the main enzymatic source of oxidative stress in cerebral vasculature, as key factors [7]. In these studies, diminished expression of tight junction proteins; reorganisation of actin cytoskeleton and the reduced viability of BBB-related major cell lines i.e. brain microvascular endothelial cells (BMEC) and astrocytes have also been shown to play pivotal roles in TNF-α-induced barrier damage [7, 8].

Activation of plasminogen-plasmin system (PPS), especially tissue plasminogen activator (tPA) and urokinase plasminogen activator (uPA) after an ischaemic stroke may initiate the process of endogenous recanalisation. Plasminogen activators convert zymogen plasminogen into plasmin which then digests the fibrin in blood clot to restore blood flow to the occluded vessels and the downstream tissue. Increases in uPA mRNA and protein expressions have also been shown in various human cell lines such as microvascular and umbilical vein endothelial cells and breast epithelial cells exposed to TNF-α [9-11]. Although elevations in intracellular calcium and NADPH oxidase activity can explain the enhanced activities of tPA and uPA during ischaemic injury, the nature of link between plasminogen activators and TNF-α with reference to BBB integrity remains unexplored [12].

Interestingly, activation of plasminogen is also implicated in the development of various inflammatory and immune responses which individually or collectively trigger extracellular proteolysis, loss of cell adhesion and disassembly of junctional complexes and consequently elicit apoptosis [10, 13]. As stimulation of apoptotic pathway by different proteins during both *in vitro* and *in vivo* ischaemic injury culminates in activation of caspase-3/7, inhibition of these enzymes with Z-VAD-FMK (carbobenzoxy-valyl-alanyl-aspartyl-[O-methyl]-fluoromethylketone) has been shown to reduce cerebral infarct volume, tight junction disruption and BBB permeability [14-16].

Protein kinase C (PKC) family of enzymes phosphorylate multiple targets on various proteins and are associated with tight junction and cytoskeletal reorganisation, endothelial barrier dysfunction, apoptosis, uPA overexpression, oxidative stress and MMP production [17-20]. Current evidence reveal that PKC-α and PKC-β isoforms play pivotal roles in TNF-α-mediated endothelial barrier dysfunction in part through elevation of Rho-A activity [18, 21, 22]. In support of these findings, inhibition of PKC-α in BMEC via its specific siRNA or inhibitor has been found to reduce the permeability of an *in vitro* model of human BBB exposed to hyperglycaemia or ischaemic injury [12, 23].

In light of the above, the current study investigates the link between PKC-α and PPS components with reference to functional alteration of *in vitro* cerebral barrier in the presence of TNF-α and attempts to scrutinise this link further in similar settings by looking at cell apoptosis, stress fibre formation and MMP activities.

2. Materials and Methods

All chemicals used in this study were from Sigma (Dorset, UK) unless otherwise stated.

2.1. Cell culture

Human brain microvascular endothelial cells (HBMEC) and human astrocytes (HA) were purchased from TCS Cell Works Ltd (Buckingham, UK) and cultured up to and including passage 6 in a humidified atmosphere (75% N_2, 20% O_2, 5% CO_2) at 37ºC in their respective specialised media (Sciencell Research Laboratories, San Diego, USA). Both media were supplemented with 1% penicillin/streptomycin mix and 1% endothelial growth supplement while 5% foetal bovine serum was added to the EC media, only 2% serum was added to the astrocyte media. To study the effects of TNF-α, in some experiments, cells grown to ~90% confluence were exposed to highly purified recombinant human TNF-α (5-10 ng/mL, R&D Systems, UK) for 6 h. In other experiments, the cells were co-treated for 6 h with TNF-α (10 ng/mL) and an inhibitor for uPA (amiloride; 2.5 μM), PKC-α (Ro-32-0432; 0.05 μM) or PKC-β (LY333531; 0.05 μM).

2.2. *In vitro* model of human BBB

An *in vitro* model of human BBB composed of HBMEC and HA was established as previously described [23-26]. Briefly, HBMEC and HA were co-cultured to full confluence in their respective specialised media successively on the inner and outer sides of the Transwell inserts (polyester membrane, 0.4 µm pore size, Corning Costar, High Wycombe, UK).

2.3. BBB experiments

The integrity and function of the BBB were assessed as before by measurements of transendothelial electrical resistance (TEER) and paracellular flux of the permeability markers, sodium fluorescein (NaF, Mw: 376 Da) and Evan's blue-labelled albumin (EBA, Mw: 67 kDa) across the *in vitro* model of human BBB [7].

2.4. Total PKC activity

Total PKC activity was measured in HBMEC lysates using the PepTag non-radioactive PKC activity assay kit (Promega, UK). Briefly, following the experimental treatments, the cells were harvested, homogenised by sonication in cold PKC extraction buffer. PKC was extracted by passing the supernatant over a 1 mL column of DEAE cellulose and eluting the PKC-containing fraction using PKC extraction buffer containing 200 mM NaCl. Samples were incubated for 30 min with a fluorescent substrate (PepTag C1 peptide), the reaction terminated by heat and separated into phosphorylated and nonphosphorylated substrates on a 0.8% agarose gel. The portion of the gel containing the phosphorylated bands was excised and solubilised at 95°C prior to addition of acetic acid to avoid solidification of the gel. The samples were placed in triplicates on a 96-well plate and absorbency was measured at 570 nm. The results were expressed in units/mL according to the calculation guidelines of the manufacturer.

2.5. Measurement of uPA activity

The levels of total uPA activity were detected by an enzyme-linked immunosorbent assay. HBMEC were grown to confluence and exposed to the outlined treatment regimes. Following the treatments, the cell culture supernatants were collected and centrifuged at 1000 g for 10 min at 4°C to remove the excess cell debris from the culture media. Briefly, samples or standard for uPA (Calbiochem) were added in duplicate to 96-well Streptavidin-coated plates (Thermo Scientific, Loughborough, UK) that had been precoated with biotinylated PAI-1 (300 ng/mL; Abcam, Cambridge, UK) and incubated for 2 h at room temperature. The plates were washed with PBS containing 0.05% Tween 20 before incubation with a primary antibody specific for uPA (rabbit; cat. no. sc-14019; 1:50; Santa Cruz Biotech, Heidelberg, Germany) for 2 h at room temperature. The plates were then washed and incubated with horseradish peroxidase-linked secondary antibodies (donkey anti-rabbit; Santa Cruz; cat. no. sc-2313; 1: 5000) and substrate solution for 20 min in the dark, respectively. The reactions were stopped by addition of stop solution (2 mM sulphuric acid) in each well and the optical densities were measured using a BMG LABTECH Omega plate reader set to 450 nm. The total uPA activity was calculated using the standard curves and normalised against the total protein concentrations as before [27].

2.6. Reverse Transcription-Polymerase Chain Reaction (RT-PCR)

Confluent HBMEC were washed with ice-cold PBS, trypsinised and centrifuged at 4ºC for 10 min at 2000 g. Total RNA extraction was performed using the GenElute mammalian total RNA kit according to the manufacturer's instructions (Sigma-Aldrich). After determining the RNA concentrations in the samples by spectrophotometry, reverse-transcription was performed using the cloned AMV first-strand cDNA synthesis kit (Invitrogen, UK). For this, total RNA (2-10 µg) was mixed with 1 µl random primer and denatured at 70ºC for 3 min before placing on ice for 2 min. cDNA preparation was initiated by adding the RNA mixture to the master reaction mix containing 0.1 mM DTT, 10 mM dNTP, 5x cDNA synthesis buffer, 1.5 µL cloned AMV RT and 1 µL RNaseOUT™. The reaction mix was incubated at 42ºC for 90 min. PCR was performed using a Mastercycle Gradient PCR device (Eppendorf Scientific). The sequences of the forward and reverse primers used to amplify uPA, uPAR, tPA and PAI-1 and 28S ribosomal RNA (internal control) are indicated in table 1. The condition for PCR reaction were as follows: initial denaturation at 94ºC for 45 sec followed by 35 cycles of denaturation at 94ºC (45 sec), annealing at 60-68ºC (1 min) and extension at 72ºC (1 min) and a final extension for (10 min) at 72ºC. The annealing temperatures used were 62°C for uPA, tPA and PAI-1, 64°C for uPAR and 68°C for 28S. The PCR products were electrophoresed through 1% agarose gels containing 0.5 µg/mL ethidium bromide. The gels were then scanned on a G Box (Syngene) and the bands were quantified using the Gene snap software from Syngene.

2.7. Immunoblotting

Equal amount of total protein samples (50-65 µg) were electrophoresed on 10% SDS-PAGE gels before transferring onto polyvinylidene fluoride membrane (GE Healthcare, Buckinghamshire, UK). The membranes were then successively incubated with a combination of primary antibodies specific for β-actin (mouse; cat no: A5441; internal control; 1:30000; Sigma, Dorset, UK) and claudin-5 (rabbit; cat no: ab53765; 1:500; Abcam, Cambridge, UK), occludin (rabbit; cat. no. sc5562; 1:650), uPA (rabbit; cat no: sc-14019; 1:400), uPAR (rabbit; cat no: sc-10815; 1:400), tPA (rabbit; cat. no. sc-15346; 1:250), PAI-1 (rabbit; cat. no. sc-8979; 1:600) and infrared dye-conjugated appropriate secondary antibodies (goat anti-mouse; cat. no. 926-68020 and goat anti-rabbit; cat. no. 926-32211; 1:30000; Li-Cor Biosciences, Cambridge, UK). All antibodies, other than those indicated

above, were from Santa Cruz Biotech (Heidelberg, Germany). The blots were visualised and analysed using the Li-Cor Odyssey infrared imaging system (Li-Cor Biosciences).

2.8. Gelatin zymography

The activities of MMP-2 and MMP-9 were measured by gelatin zymography. Equal amounts of culture media used to grow cells (5-10 µL) or total cellular protein (20-70 µg/mL) were electrophoresed on 10% SDS-PAGE gel containing 0.1% gelatin. The positive controls for MMP-2 and MMP-9 were also run on each gel. The gels were then washed for 30 min in 2.5% Triton X-100 and incubated overnight at 37ºC in a buffer containing 50 mM Tris (pH 7.5), 10 mM $CaCl_2$, 50 mM NaCl and 0.05% Brij-35 (Calbiochem, UK). The gels were then stained for 2 h in 0.1% Comassie Brilliant Blue-G dye containing 25% methanol and 5% acetic acid and then destained for a minimum of 1 h in 50% methanol and 25% acetic acid. Bands were visualised and quantified using Li-Cor Odyssey infrared imaging system and the readings were normalised to "mg protein".

2.9. F-actin staining

The presence of stress fibres was assessed through F-actin staining in cells cultured to ~80% confluence on sterile glass coverslips and exposed to normal and experimental conditions. For this, the cell culture media were carefully aspirated and the cells were fixed and permeabilised in 4% paraformaldehyde/ PBS for 20 min and 0.1 % Triton X-100/ PBS for 15 min, respectively. Cells were then blocked with 10% BSA/PBS for 30 min before staining actin microfilaments via rhodamine-labelled phalloidin dye (5 U/mL) for 30 min at room temperature away from light. The coverslips were washed and incubated in the dark with 4',6-diamidino-2-phenylindole (DAPI) for 5 min at room temperature. The excess DAPI was removed and the coverslips were mounted using glycerol/PBS (3:1) and the edges were sealed by a nail polish. Slides were viewed by Zeiss Axio Observer fluorescence microscope.

2.10. TUNEL staining

TUNEL staining was performed using a DeadEnd colourimetric TUNEL system detection kit as per the manufacturer's instructions (Promega, UK). Briefly, HBMEC cultured to ~90% confluence on glass coverslips were fixed and permeabilised as above before equilibrating for 10 min in a solution containing potassium cacodylate (200 mM), Tris-HCl (25 mM),

dithiothreitol (0.2 mM), BSA (250 mg/L) and cobalt chloride (2.5 mM). To allow end-labelling to occur, the coverslips were then incubated for 60 min with recombinant terminal deoxynucleotidyl transferase (rTdT) reaction mix containing equilibrium buffer (98 µL), biotinylated nucleotide mix (1 µL) and rTDT enzyme (1 µL). The reaction was then stopped by dipping coverslips into 20x SSC buffer before blocking and staining them with 0.3% H_2O_2 and horseradish peroxidase-labelled streptavidin (500 mg/L; 1:500), respectively. TUNEL-positive cells were then detected via diaminobenzidine which gave the dark brown staining to the apoptotic cells. Cells were viewed under Zeiss Axio Observer microscope and counted (TUNEL-positive vs total) from 3 different fields per coverslip before calculating mean values for these areas.

2.11. Caspase-3/7 activity

Caspase-3/7 activity assay was performed using Apo-ONE homogeneous caspase-3/7 kit (Promega, UK). Briefly, cells grown to ~95% confluence in 96-well plates were subjected to experimental conditions. Following the treatments, 100 µL of media was removed from each well and replaced by 100 µL of caspase-3/7 assay buffer containing the non-flourescent caspase substrate rhodamine 110,bis-(N-CBZ-L-aspartyl-L-glutamyl-L-valyl-L-aspartic acid amide; Z-DEVD-R110) to initiate the reaction. The 96-well plates were then frozen at -80°C overnight. On the following day plates were thawed on a plate shaker for 2 h before reading the fluorescence. The cleavage of the non-fluorescent caspase substrate by caspase-3/7 produced the fluorescent rhodamine-110 which was read at excitiation wavelength 485 nm and emission wavelength 520 nm using BMG LABTECH Omega plate reader. Blanks were subtracted from the readings which then were normalised to "mg protein".

2.12. Small interfering RNA (siRNA) transfection

Cells cultured to ~70% confluence were washed with sterile PBS to remove traces of serum and antibiotics. The transfection medium was prepared by diluting the DharmaFECT siRNA transfection reagent 4 (containing 5-50 nM ON-TARGET plus SMART pool siRNA oligonucleotides against human PKC-α) in serum-free media. HBMEC were incubated with 2 mL of transfection media for 24 h. The next day the transfection medium was aspirated and fresh ECM was added. On day three, transfection was repeated after which the cells were exposed to relevant experimental conditions. Similar experiments were carried out with non-

targeting siRNA pool. Ultimately, the cells were homogenised and the transfection efficiency was confirmed by Western analyses of PKC-α in the sample. The sequences of the oligonucleotides used in PKC-α SMARTpool were: UCACUGCUCUAUGGACUUA, GAAGGGUUCUCGUAUGUCA, UUAUAGGGAUCUGAAGUUA and UAAGGAACCA CAAGCAGUA.

2.13. Cell viability assay

To detect cytotoxic effects of different treatment regimens on cells, viability assays were carried out regularly. Briefly, an aliquot of cells was mixed with 0.1% Trypan blue for 5 min before counting 100 cells using a light microscope to calculate the percentage viability.

2.14. Statistical analysis

Data are presented as mean±SEM. Statistical analyses were conducted using IBM SPSS statistics 20.0 software package. Mean values were compared by Student's two-tailed *t*-test and one-way analysis of variance followed by Dunnett's *post-hoc* analysis. *P*<0.05 was considered to be significant in all the experiments.

3. Results

3.1. TNF-α upregulates the mRNA and protein expressions of all PPS components

Exposure of HBMEC to two different concentrations of TNF-α (5-10 ng/mL) for 6 h significantly increased uPA, uPAR, PAI-1 and tPA mRNA and protein expressions compared to control cells (Fig. 1A-D).

3.2. TNF-α perturbs BBB integrity and function

TNF-α (10 ng/mL) significantly compromised the integrity and function of the selected *in vitro* model of human BBB as evidenced by marked decreases in TEER values and concomitant increases in flux of both low and high molecular weight paracellular permeability markers, namely NaF (376 Da) and EBA (67 kDa). However, while inhibition of uPA by amiloride (2.5 μM) attenuated the extent of TNF-α-induced barrier damage, application of amiloride on its own had no profound effect on barrier integrity or function (Fig. 2A-C).

3.3. Effects of TNF-α on MMP and total PKC activities

Exposure of HBMEC to TNF-α (10 ng/mL) for 6 h led to dramatic increases in both total PKC and extracellular MMP-2 activities where no difference in intracellular MMP-2 activity was observed. Interestingly, while amiloride neutralised TNF-α-mediated increases in extracellular MMP-2 activity, it had no effect on that of the total PKC (Fig. 3A-C).

3.3. TNF-α augments uPA activity through activation of protein kinase C-α/β

TNF-α caused a significant increase in endothelial cell uPA activity which was diminished by the inhibitor of PKC-β (0.05 μM) and normalised by that of PKC-α (0.05 μM). The use of either inhibitor alone did not significantly affect uPA activity (Fig. 4A). Although PKC-α inhibitor used in the current study displays a high specificity for this particular isoform, it has also been reported to suppress the activity of other PKC isoforms albeit with substantially lower IC_{50} values. To reveal whether, and to what extent, PKC-α contributes to TNF-α-mediated disruption of the BBB and regulates the mechanisms associated with this phenomenon, PKC-α specific siRNA was employed to switch off its transcriptional activity. Subsequent immunoblotting tested the efficacy of transfection experiments in that non-target siRNAs were used as controls (Fig. 4B).

3.4. Silencing PKC-α attenuates the effects of TNF-α on PPS components and MMP activity

Knockdown of PKC-α gene in HBMEC slightly but significantly reduced TNF-α-mediated elevations observed in uPA, tPA, uPAR and PAI-1 protein expressions, indicating that PKC-α acts upstream to all PPS components. Similar to these, transfection with PKC-α siRNA also significantly reduced both extracellular and intracellular MMP-2 activities compared to cells transfected with non-target siRNA (Figure 5A-F).

3.5. PKC-α is involved in the deleterious effects of TNF-α on tight junction protein expressions, BMEC viability and cytoskeleton

Treatments with TNF-α substantially diminished the level of claudin-5 and occludin protein expressions in BMEC. Suppression of PKC-α activity abolished these decreases and also produced selective increases in claudin-5 expression (Fig. 6A-B). Inhibition of PKC-α also

decreased the levels of TNF-α-induced DNA fragmentation and pro-apoptotic caspase-3/7 activities in BMEC where formation of stress fibres also appeared to decrease (Fig. 7A-D).

3.6. Effects of PKC-α silencing on BBB integrity and function

As indicated above, TNF-α markedly impaired *in vitro* barrier integrity and function as proven by reduced TEER and increased flux of NaF and EBA, respectively. Establishment of co-cultures with BMEC transfected with PKC-α siRNA significantly attenuated the effects of TNF-α on BBB integrity and function (Figure 8A-C).

4. Discussion

Spontaneous cerebral artery recanalisation after an acute ischaemic attack is observed in almost a quarter of patients and is closely correlated with better survival rates and outcome largely due to the presence of still salvageable penumbral tissue during the early phases of stroke [28]. Although useful for post-ischaemic endogenous recanalisation, activation of PPS involving uPA, its specific receptor uPAR and tPA is also closely implicated in the initiation and progression of various neurovascular complications including degradation of basement membrane and BBB failure [10, 13]. Considering the excessive release of inflammatory cytokines during an ischaemic attack and in light of our recent studies exhibiting the barrier-disruptive function of TNF-α, this study examined the putative involvement(s) of PPS components and associated downstream mechanisms in TNF-α-mediated BBB damage [7, 8]. In this context, our initial studies assessing the effects of two pathologically relevant concentrations of TNF-α (5-10 ng/mL) have shown significant increases in mRNA and protein levels of all PPS components. Similar specific increases in uPA mRNA and protein levels have previously been reported in human foreskin microvascular endothelial cells exposed to TNF-α in hypoxic conditions [11]. The transcriptional and translational increases in uPA appeared to be reflective of that seen in its activity. Given that a selective increase in tPA activity failed to alter BBB integrity and function under normoxic and ischaemic conditions, TNF-α does not modulate tPA activity and a significant proportion of tPA in brain microvessels appears to exist in an inactive complex with PAI-1, the current study focussed solely on uPA activity [27, 29, 30]. Furthermore, it is anticipated that TNF-α-mediated increases observed in endothelial cell PAI-1 mRNA and protein expressions would tilt the balance from free tPA to tPA/PAI-1 complex even further and may actually provide a

compensatory mechanism against its potentiating impact on plasminogen activator activity in inflammatory settings.

Using an in vitro model of human BBB consisting of BMEC and HA, this study has shown that inhibition of uPA has dramatically attenuated, but not neutralised, the detrimental effects of TNF-α on barrier integrity and function. Marked increases in TEER and concomitant decreases in paracelluar flux verified this notion and pinpointed the involvement of other mechanisms in this phenomenon. Previous studies scrutinising the barrier-protective effects of targeting uPA (by amiloride) or uPAR (by anti-uPAR antibody) activity have attributed the observed benefits to concurrent attenuations of endothelial MMP-2 and NADPH oxidase activities in ischaemic conditions [27, 31, 32].

NADPH oxidases make up a family of superoxide anion-generating enzymes that are induced by coupling of its catalytic subunit, Nox with other subunits e.g. p22-phox and p47-phox and act as downstream mediators of various PKC isoforms. Out of the seven isoforms of Nox identified to date, only Nox2 appears to play a tangible role after stroke [33]. Indeed, a steady increase in Nox2 protein expression in penumbral endothelial cells and microglia has been observed until day three following middle cerebral artery occlusion and Nox2-deficient mice develop considerably smaller cerebral infarcts after a similar insult [34, 35]. Similarly, while increases have been reported in Nox4 and Nox1 protein expressions in human and rodent cerebral vessels after stroke, their roles remain rather obscure in that there are reports showing that knockdown of Nox1 or Nox4 gene in mice led to or failed to show neuroprotection [36].

MMPs are a family of zinc-dependent endopeptidases that degrade extracellular matrix and basement membrane proteins while promoting BBB malfunction by severely disrupting brain endothelial cell anchoring and matrix-endothelial cell signalling [37-39]. The relevance of over or uncontrolled expression of MMPs to TNF-α-induced cerebral barrier and tissue damage has been reported in various *in vitro* and *in vivo* studies [40-42]. Overactivation of various MMP isoforms, in particular MMP-1, -2, -3 and -9 has subsequently been connected to TNF-α-induced BBB hyperpermeability [7, 43-45]. In support of this, the intracerebral injection of TNF-α into rat brain was shown to induce MMP-9 activation and BBB disruption where inhibition of MMP by a synthetic MMP inhibitor, Batimastat, markedly reduced the capillary permeability [45]. In accordance with these data, the current study also shows a

significant but selective increase in extracellular, but not in intracellular, MMP-2 activity in TNF-α-treated HBMEC. Although the inability of TNF-α to augment basal intracellular MMP-2 activity may in part explain this, excretion of intracellular MMPs to extracellular space for activation to combat cellular stress like TNF-α is also likely to play a role. As most MMPs respond to the early stage of stimuli at transcriptional levels and are synthesised as intracellular isoforms [46], our data suggest that treatments with TNF-α for 6 h adequately accelerate MMP-2 gene transcription and ensuing secretion from cytosol.

As expected from its BBB-protective effects, amiloride effectively neutralised the effects of TNF-α on extracellular MMP-2 protein expression. However, it displayed no impact on intracellular isoform which was in contrast to its equally suppressive effects on both MMP-2 isoforms in experimental settings of ischaemic injury where inhibition of PKC-α was also proven to be equally effective [27]. Interestingly, in the present study the inhibition of PKC-α via specific siRNAs also abolished the TNF-α-mediated increases seen in extracellular MMP-2 activity and diminished the level of intracellular isoform below the levels seen in TNF-α-untreated control cells. Similar decreases in pro-MMP-2 and membrane type 1-MMP expressions were previously obtained with PKC-α inhibition in bovine pulmonary artery smooth muscle cells subjected to TNF-α [20]. Collectively, these data suggest PKC-α as a better therapeutic target in preventing TNF-α-evoked cerebral barrier damage.

Considering that TNF-α-mediated increases in human dental pulp and umbilical vein endothelial cell uPA levels were regulated by PKC [19, 47], we investigated the specific correlation between HBMEC uPA activity and two different PKC isoforms known to have profound relevance to BBB integrity i.e. PKC-α and PKC-β. Although inhibition of both isoforms significantly mitigated uPA activity, the magnitude of decreases appeared to be grater with PKC-α inhibition. Hence, this particular isoform was targeted during the rest of the study using its specific siRNA. Taken together with the inability of amiloride to diminish TNF-α-induced total PKC activity, these results confirmed the upstream localisation of PKC to uPA similar to a study revealing attenuation of TNF-α-induced uPA overexpression in human umbilical vein endothelial cells by three different PKC inhibitors, namely H-7, staurosporine, and calphostin C [19].

Like MMP-2 and uPA, specific targeting of PKC-α activity by its siRNA also effectively decreased the protein expression of other PPS components. As non-targeting siRNAs failed

to influence the TNF-α-triggered increases in MMP-2-activity and PPS protein expressions, it is safe to state that inhibition of PKC-α subdues the pathways downstream to uPA and vitiates their deleterious effects on the cerebral barrier. Indeed, significant attenuation of permeability across co-cultures established by HBMEC transfected with PKC-α siRNA confirmed this assumption [18, 22]. Enhanced expression or normalisation of claudin-5 and occludin, tight junction proteins, by PKC-α knockdown in part accounts for its barrier-protective effects [48]. Considering that silencing of PKC-α led to elevation of both protein expressions in HBMEC regardless of their exposure to TNF-α, it is plausible to speculate that the observed increases may largely stem from an increased translational activity rather than prevention of their degradation or redistribution. Understanding how tight junctions may become vulnerable to damage by TNF-α may lead to efficacious prevention and treatment of ischaemic stroke-mediated development of brain oedema, the main cause of death within the first week after a stroke. The functional relevance between the level of tight junction proteins and the cerebral barrier integrity has previously been shown in a model of transient ischaemic stroke where reperfusion injury-evoked BBB openings were closely linked to the diminished expressions of occludin, claudin-5 and ZO-1 [49].

Increases in actin stress fibre formation with TNF-α have previously been associated with endothelial gap formation, tight junction protein disassembly and subsequent promotion of endothelial barrier dysfunction [22]. In this study, HBMEC grown under normal conditions displayed thick cortical F-actin staining and had spindle-shaped morphology. In contrast, cells exposed to TNF-α possessed elongated morphology and thick stress fibres traversing the cells like those reported in human umbilical vein endothelial cells incubated with TNF-α for 8-24 hours [50]. Once formed, stress fibres produce a tensile centripetal force to pull junctional protein inward to disrupt junctional complex and form paracellular openings. Although several mechanisms, including activation of vascular endothelial growth factor and NF-κB are implicated in ischaemic injury-mediated junctional breakdown, TNF-α-mediated overactivation of PKC-α has been coupled to cytoskeletal reorganisation in mouse BMEC [22, 51, 52]. In the present study, restoration of normal cellular morphology and attenuation of stress fibres formation in HBMEC by PKC-α siRNA in addition to protection of *in vitro* barrier function add further weight to the findings of the latter study mentioned above.

Enhanced apoptosis of endothelial cells triggered by TNF-α is also implicated in cerebral barrier dysfunction [32, 53]. Indeed, marked increases in TUNEL staining, a hallmark of DNA fragmentation and pro-apoptotic caspase-3/7 activities in HBMEC support this notion. Activation of caspase-3/7 by TNF-α has previously been linked with dissolution of tight junctions and shown to induce human brain endothelial cell apoptosis and paracellular permeability [54]. Significant weakening of DNA fragmentation and caspase-3/7 activities by PKC-α knockdown, but not non-targeting siRNAs, alongside the preservation of cerebral barrier integrity indicate the disruptive role of HBMEC apoptosis in inflammatory cytokine-induced barrier failure. The data also further confirm the therapeutic value of targeting PKC-α in clinical settings associated with exaggerated synthesis or release of pro-inflammatory cytokines like TNF-α while suggesting the concomitant involvement of other TNF-α-induced mediators in the process. Although not studied here, it is probable that PKC-α-induced translocation of an active form of pro-apoptotic Bax protein into the outer mitochondrial membrane and subsequent increases in cytochrome *C* and reactive oxygen species production along with mitochondrial network fragmentation may also contribute to HBMEC apoptosis [55, 56]. Previously reported requirements for increases in PKC-α protein expression or activity to enhance glioma and breast cancer cell survival necessitate the in depth investigation of downstream mechanisms involved. However, the overt differences in characteristics of these cell lines, namely endothelial versus cancerous cells cannot be dismissed in this context [57, 58].

There are some limitations to this study. Despite the existence of a well-documented cross-talk between HBMEC and astrocytes in the current model, the absence of other components of the neurovascular unit i.e. neurons, pericytes and microglia that affect the integrity and function of the BBB and the CNS as a whole should be noted here [7, 8]. Hence, it is essential to confirm the results presented in this study in *in vivo* settings by using an animal model of transient ischaemic stroke accompanied by excessive release of pro-inflammatory cytokine TNF-α. It is noteworthy here that other PKC isoforms, namely nPKC-θ and aPKC-ζ that appear to regulate tight junctional assembly and BBB integrity during experimental hypoxia and posthypoxic oxygenation may also be involved in the barrier-disruptive effects of TNF-α [59]. It is also noteworthy that TNF-α-mediated induction of pro-inflammatory cytokine IL-6 and its receptor GP130 in BMEC may also contribute to its barrier-disruptive effects due to downregulation of both tight and adherens junctions [60].

In conclusion, the current study reveals that excessive bioavailability of TNF-α severely disrupts the integrity and function of an *in vitro* model of human BBB through successive activations of PKC-α and MMP-2 and associated induction of uPA alongside the other PPS components, tight junctional complex disintegration, endothelial cell structural malformation and apoptosis. Since inhibition of PKC-α activity can effectively negate the deleterious effects of TNF-α on HBMEC, targeting this particular signalling pathway may be of therapeutic value in ischaemic stroke and other cerebrovascular diseases accompanied by abundant release of pro-inflammatory cytokines, notably TNF-α.

Disclosures

Sources of funding

References

[1]   T. Nishioku, J. Matsumoto, S. Dohgu, N. Sumi, K. Miyao, F. Takata, H. Shuto, A. Yamauchi, Y. Kataoka, Tumor Necrosis Factor-alpha Mediates the Blood-Brain Barrier Dysfunction Induced by Activated Microglia in Mouse Brain Microvascular Endothelial Cells, J. of Pharmacol. Sci. 112 (2010) 251-254.

[2]   P. Ballabh, A. Braun, M. Nedergaard, The blood-brain barrier: an overview: Structure, regulation, and clinical implications, Neurobiol. Dis.16 (2004) 1-13.

[3]   K. Hayashi, S. Nakao, R. Nakaoke, S. Nakagawa, N. Kitagawa, M. Niwa, Effects of hypoxia on endothelial/pericytic co-culture model of the blood-brain barrier, Regul. Peptides. 123 (2004) 77-83.

[4]   K.E. Sandoval, K.A. Witt, Blood-brain barrier tight junction permeability and ischemic stroke, Neurobiol. Dis. 32 (2008) 200-219.

[5]   A.J. Farrall, J.M. Wardlaw, Blood–brain barrier: Ageing and microvascular disease – systematic review and meta-analysis, Neurobiol. Aging. 30 (2009) 337-352.

[6]   F.L. Cardoso, D. Brites, M.A. Brito, Looking at the blood-brain barrier: Molecular anatomy and possible investigation approaches, Brain. Res. Rev. 64 (2010) 328-363.

[7]   Z. Abdullah, U. Bayraktutan, NADPH oxidase mediates TNF-alpha-evoked *in vitro* brain barrier dysfunction: roles of apoptosis and time, Mol Cell. Neurosci. 61 (2014) 72-84.

[8]   Z. Abdullah, K. Rakkar, P.M.W. Bath, U. Bayraktutan, Inhibition of TNF-alpha protects in vitro brain barrier from ischaemic damage, Mol. Cell. Neurosci. 69 (2015) 65-79.

[9]   M.J. Niedbala, M.S. Picarella, Tumor necrosis factor induction of endothelial cell urokinase-type plasminogen activator mediated proteolysis of extracellular matrix and its antagonism by gamma-interferon, Blood 79 (1992) 678-687.

[10]   M.-J. Kim, D.-H. Kim, H.-K. Na, Y.-J. Surh, TNF-α induces expression of urokinase-type plasminogen activator and β-catenin activation through generation of ROS in human breast epithelial cells, Biochem. Pharmacol. 80 (2010) 2092-2100.

[11]   M.E. Kroon, P. Koolwijk, B. van der Vecht, V.W.M. van Hinsbergh, Urokinase receptor expression on human microvascular endothelial cells is increased by hypoxia: implications for capillary-like tube formation in a fibrin matrix, Blood 96 (2000) 2775-2783.

[12]   K. Rakkar, U. Bayraktutan, Increases in intracellular calcium perturb blood-brain barrier via protein kinase C-alpha and apoptosis, BBA-Mol. Basis Dis. 1862 (2015) 56-71.

[13]   A. Mondino, F. Blasi, uPA and uPAR in fibrinolysis, immunity and pathology, Trends Immunol. 25 (2004) 450-455.

[14]   S.-R. Lee, E.H. Lo, Interactions Between p38 Mitogen-Activated Protein Kinase and Caspase-3 in Cerebral Endothelial Cell Death After Hypoxia-Reoxygenation, Stroke 34 (2003) 2704-2709.

[15]   C.M. Zehendner, L. Librizzi, M. de Curtis, C.R.W. Kuhlmann, H.J. Luhmann, Caspase-3 Contributes to ZO-1 and Cl-5 Tight-Junction Disruption in Rapid Anoxic Neurovascular Unit Damage, PLoS ONE 6 (2011) e16760.

[16]   S. Park, M. Yamaguchi, C. Zhou, J.W. Calvert, J. Tang, J.H. Zhang, Neurovascular Protection Reduces Early Brain Injury After Subarachnoid Hemorrhage, Stroke 35 (2004) 2412-2417.

[17]   C.A. Aveleira, C.M. Lin, S.F. Abcouwer, A.F. Ambrosio, D.A. Antonetti, TNF-alpha Signals Through PKC zeta/NF-kappa B to Alter the Tight Junction Complex and Increase Retinal Endothelial Cell Permeability, Diabetes 59 (2010) 2872-2882.

[18]   T. Ferro, P. Neumann, N. Gertzberg, R. Clements, A. Johnson, Protein kinase C- α mediates endothelial barrier dysfunction induced by TNF- α, Am. J. Physiol. Lung Cell. Mol. Physiol. 278 (2000) L1107-L1117.

[19]   M.J.S.-P.M. Niedbala, Role of protein kinase C in tumor necrosis factor induction of endothelial cell urokinase-type plasminogen activator, Blood 81 (1993) 2608-2617.

[20]   S. Roy, T. Chakraborti, A. Chowdhury, S. Chakraborti, Role of PKC- α in NF-kB-MT1-MMP-mediated activation of proMMP-2 by TNF-α in pulmonary artery smooth muscle cells, J. Biochem. 153 (2013) 289-302.

[21]   T.J. Ferro, D.M. Parker, L.M. Commins, P.G. Phillips, A. Johnson, Tumor necrosis factor-alpha activates pulmonary artery endothelial protein kinase C, Am. J. Physiol. 264 (1993) L7-L14.

[22]   J. Peng, F. He, C. Zhang, X. Deng, F. Yin, Protein kinase C- α signals P115RhoGEF phosphorylation and RhoA activation in TNF-α-induced mouse brain microvascular endothelial cell barrier dysfunction, J. Neuroinflamm. 8 (2011) 28.

[23]   B. Shao, U. Bayraktutan, Hyperglycaemia promotes cerebral barrier dysfunction through activation of protein kinase C-β, Diabetes Obes. Metab. 15 (2013) 993-999.

[24]   C. Allen, K. Srivastava, U. Bayraktutan, Small GTPase RhoA and Its Effector Rho Kinase Mediate Oxygen Glucose Deprivation-Evoked In Vitro Cerebral Barrier Dysfunction, Stroke (2010).

[25]   C.L. Allen, U. Bayraktutan, Antioxidants attenuate hyperglycaemia-mediated brain endothelial cell dysfunction and blood–brain barrier hyperpermeability, Diabetes Obes. Metab. 11 (2009) 480-490.

[26] K. Srivastava, B. Shao, U. Bayraktutan, PKC-[beta] exacerbates in vitro brain barrier damage in hyperglycemic settings via regulation of RhoA/Rho-kinase/MLC2 pathway, J. Cereb. Blood Flow Metab. (2013).

[27] K. Rakkar, K. Srivastava, U. Bayraktutan, Attenuation of urokinase activity during experimental ischaemia protects the cerebral barrier from damage through regulation of matrix metalloproteinase-2 and NAD(P)H oxidase, Eur. J. Neurosci. 39 (2014) 2119-2128.

[28] J.-H. Rha, J.L. Saver, The Impact of Recanalization on Ischemic Stroke Outcome: A Meta-Analysis, Stroke 38 (2007) 967-973.

[29] V.W. van Hinsbergh, E.A. van den Berg, W. Fiers, G. Dooijewaard, Tumor necrosis factor induces the production of urokinase-type plasminogen activator by human endothelial cells, Blood 75 (1990) 1991-1998.

[30] B.V. Zlokovic, Antithrombotic, procoagulant, and fibrinolytic mechanism in cerebral circulation: implications for brain injury and protection, Neurosurg. Focus 15 (1997) 6.

[31] S. Nakagawa, M.A. Deli, H. Kawaguchi, T. Shimizudani, T. Shimono, A. Kittel, K. Tanaka, M. Niwa, A new blood-brain barrier model using primary rat brain endothelial cells, pericytes and astrocytes, Neurochem. Int. 54 (2009) 253-263.

[32] D. Yang, P. Xie, S. Guo, H. Li, Induction of MAPK phosphatase-1 by hypothermia inhibits TNF-α-induced endothelial barrier dysfunction and apoptosis, Cardiovasc. Res. 85 (2010) 520-529.

[33] D. Cosentino-Gomes, N. Rocco-Machado, J.R. Meyer-Fernandes, Cell Signaling through Protein Kinase C Oxidation and Activation, Int. J. Mol. Sci. 13 (2012) 10697-10721.

[34] H. Chen, Y.S. Song, P.H. Chan, Inhibition of NADPH Oxidase is Neuroprotective after Ischemia-Reperfusion, J. Cereb. Blood Flow Metab. 29 (2009) 1262-1272.

[35] S.P. Green, B. Cairns, J. Rae, C. Errett-Baroncini, J.-A.S. Hongo, R.W. Erickson, J.T. Curnutte, Induction of gp91-phox, a Component of the Phagocyte NADPH Oxidase, in Microglial Cells during Central Nervous System Inflammation, J. Cereb. Blood Flow Metab. 21 (2001) 374-384.

[36] T. Kahles, R.P. Brandes, Which NADPH Oxidase Isoform Is Relevant for Ischemic Stroke? The Case for Nox 2, Antioxid. Redox Signal.18 (2013) 1400-1417.

[37] S.L. Leib, D. Leppert, J. Clements, M.G. Tauber, Matrix Metalloproteinases Contribute to Brain Damage in Experimental Pneumococcal Meningitis, Infection and Immunity, Infect. Immun. 68 (2000) 615-620.

[38] W.C. Parks, C.L. Wilson, Y.S. Lopez-Boado, Matrix metalloproteinases as modulators of inflammation and innate immunity, Nat. Rev. Immunol. 4 (2004) 617-629.

[39] P.M. Carvey, B. Hendey, A.J. Monahan, The blood-brain barrier in neurodegenerative disease: a rhetorical perspective, J. Neurochem. 111 (2009) 291-314.

[40] R. Reyes, M. Guo, K. Swann, S.U. Shetgeri, S.M. Sprague, D.F. Jimenez, C.M. Barone, Y. Ding, Role of tumor necrosis factor- α and matrix metalloproteinase-9 in blood-brain barrier disruption after peripheral thermal injury in rats, J. Neurosurg. 110 (2009) 1218-1226.

[41] M. Tsuge, K. Yasui, T. Ichiyawa, Y. Saito, Y. Nagaoka, M. Yashiro, N. Yamashita, T. Morishima, Increase of tumor necrosis factor-α in the blood induces early activation of matrix metalloproteinase-9 in the brain, Microbiol. Immun. 54 (2010) 417-424.

[42] P. Zeni, E. Doepker, U.S. Topphoff, S. Huewel, T. Tenenbaum, H.-J. Galla, MMPs contribute to TNF-α-induced alteration of the blood-cerebrospinal fluid barrier in vitro, Am J Physiol. Cell Physiol. 293 (2007) C855-C864.

[43] A.G. Braundmeier, R.A. Nowak, Cytokines Regulate Matrix Metalloproteinases in Human Uterine Endometrial Fibroblast Cells Through a Mechanism That Does Not Involve Increases in Extracellular Matrix Metalloproteinase Inducer, Am. J. Reprod. Immunol. 56 (2006) 201-214.

[44] Y.P. Han, T.L. Tuan, H. Wu, M. Hughes, W.L. Garner, TNF-alpha stimulates activation of pro-MMP2 in human skin through NF-(kappa)B mediated induction of MT1-MMP, J. Cell Sci. 114 (2001) 131-139.

[45] G.A. Rosenberg, E.Y. Estrada, J.E. Dencoff, W.G. Stetler-Stevenson, Tumor necrosis factor-α-induced gelatinase B causes delayed opening of the blood-brain barrier: an expanded therapeutic window, Brain Res. 703 (1995) 151-155.

[46] H. Nagase, R. Visse, G. Murphy, Structure and function of matrix metalloproteinases and TIMPs, Cardiovasc. Res. 69 (2006) 562-573.

[47] H. Hashizume, N. Kamio, S. Nakao, K. Matsushima, H. Sugiya, Protein Kinase C Synergistically Stimulates Tumor Necrosis Factor- α-Induced Secretion of Urokinase-Type Plasminogen Activator in Human Dental Pulp Cells, J. Physiol. Sci 58 (2008) 83-86.

[48] H. Clarke, N. Ginanni, K.V. Laughlin, J.B. Smith, G.R. Pettit, J.M. Mullin, The transient increase of tight junction permeability induced by bryostatin 1 correlates with rapid downregulation of protein kinase C-alpha., Exp. Cell Res. 261 (2000) 239-249.

[49] S. H. Jiao, Z. Wang, Y. Liu, P. Wang, Y. Xue, Specific role of tight junction proteins Claudin-5, Occludin, and ZO-1 of the blood-brain barrier in a focal cerebral ischemic insult., J. Mol. Neurosci. 44 (2011) 130-139.

[50] J.A.G. McKenzie, A.J. Ridley, Roles of Rho/ROCK and MLCK in TNF-α-induced changes in endothelial morphology and permeability, J. Cell. Physiol. 213 (2007) 221-228.

[51] K.S. Mark, T.P. Davis, Cerebral microvascular changes in permeability and tight junctions induced by hypoxia-reoxygenation, Am. J. Physiol. Heart Circ. Physiol. 282 (2002) H1485-H1494.

[52] N. van Bruggen, H. Thibodeaux, J.T. Palmer, W.P. Lee, L. Fu, B. Cairns, D. Tumas, R. Gerlai, S.-P. Williams, M.v.L. Campagne, N. Ferrara, VEGF antagonism reduces edema formation and tissue damage after ischemia/reperfusion injury in the mouse brain, J. Clin. Invest.104 (1999) 1613-1620.

[53] I. Petrache, A.D. Verin, M.T. Crow, A. Birukova, F. Liu, J.G.N. Garcia, Differential effect of MLC kinase in TNF-α-induced endothelial cell apoptosis and barrier dysfunction, Am. J. Physiol. Lung Cell. Mol. Physiol. 280 (2001) L1168-L1178.

[54] M.A. Lopez-Ramirez, R. Fischer, C.C. Torres-Badillo, H.A. Davies, K. Logan, K. Pfizenmaier, D.K. Male, B. Sharrack, I.A. Romero, Role of Caspases in Cytokine-Induced Barrier Breakdown in Human Brain Endothelial Cells, J. Immunol.189 (2012) 3130-3139.

[55] R.D. Silva, S. Manon, J. Goncalves, L. Saraiva, M. Corte-Real, Modulation of Bax mitochondrial insertion and induced cell death in yeast by mammalian protein kinase Cα, Exp. Cell Res. 317 (2011) 781-790.

[56] B. Shao, U. Bayraktutan, Hyperglycaemia promotes human brain microvascular endothelial cell apoptosis via induction of protein kinase C-beta(I) and prooxidant enzyme NADPH oxidase, Redox Biology 2 (2014) 694-701.

[57] A.J. Cameron, K.J. Procyk, M. Leitges, P.J. Parker, PKC alpha protein but not kinase activity is critical for glioma cell proliferation and survival, Int. J. Cancer 123 (2008) 769-779.

[58] X.F. Le, M. Marcelli, A. McWatters, B. Nan, G. Mills, C. O'Brian, R.J. Bast, Heregulin-induced apoptosis is mediated by down-regulation of Bcl-2 and activation of caspase-7 and is potentiated by impairment of protein kinase C alpha activity, Oncogene 20 (2001) 8258-8259.

[59] C.L. Willis, D.S. Meske, T.P. Davis, Protein Kinase C Activation Modulates Reversible Increase in Cortical Blood-Brain Barrier Permeability and Tight Junction Protein Expression during Hypoxia and Posthypoxic Reoxygenation, J. Cereb. Blood Flow Metab. 30 (2010) 1847-1859.

[60] K.D. Rochfort, L.E. Collins, A. McLoughlin, P.M. Cummins, Tumour necrosis factor-α-mediated disruption of cerebrovascular endothelial barrier integrity in vitro involves the production of proinflammatory interleukin-6, J. Neurochem. 136 (2016) 564-572.

Figure Legends

Figure 1 – 2 columns

TNF-α increased mRNA and protein expressions of all plasminogen-plasmin system coponents. HBMECs were exposed to TNF-α (5-10 ng/mL) for 6 h before measurement of uPA (A), uPAR (B), tPA (C) and PAI-1 (D) mRNA and protein expressions. The readings were normalised to the levels of 28S rRNA for mRNA and β-actin for protein expressions, respectively. TNF-α caused significant increases in mRNA and protein levels of all PPS components in HBMEC as compared with controls. Data are expressed as mean±SEM from 9 different experiments. *p<0.05 vs control, †p<0.05 vs TNF-α (5 ng/mL).

Figure 2 – 1 column

Amiloride ameliorated the detrimental effects of TNF-α on BBB integrity and function. HBMEC-HA co-cultures were exposed to 6 h TNF-α (10 ng/mL) in the absence or presence of an inhibitor for uPA (amiloride, 2.5 μmol/L). TNF-α significantly impaired BBB integrity and function as shown by a reduction in TEER (A) and increases in NaF (B) and EBA (C) flux volumes, which were prevented by amiloride treatment. Data are expressed as mean±SEM from 12 different experiments. *p<0.05 vs control, †p<0.05 vs TNF-α (10 ng/mL), #p<0.05 vs amiloride + TNF-α.

Figure 3 – 1 column

TNF-α enhanced MMP-2 and total PKC activities. TNF-α (10 ng/mL) significantly increased total PKC activity and extracellular pro-MMP-2 levels in endothelial cells without affecting that of intracellular MMP-2 (A-C). Inhibition uPA activity by amiloride normalised extracellular pro-MMP-2 levels but appeared to be ineffective in the case of total PKC activity. Data are expressed as mean±SEM from 12 different experiments. *p<0.05 vs control, †p<0.05 vs TNF-α (10 ng/mL), #p<0.05 vs amiloride + TNF-α.

Figure 4 – 1 cloumn

Inhibition of PKC-α and PKC-β attenuated the effects of TNF-α on total uPA activity. HBMEC were exposed to 6 h TNF-α (10 ng/mL) in the absence or presence of an inhibitor

for PKC-α (Ro-32-04-32, 0.05 μM) or PKC-β (LY333531, (0.05 μM). Both inhibitors significantly reduced TNF-α-induced increases in endothelial cell total uPA activity (A). Knockdown of PKC-α by specific siRNA reduced PKC-α protein expression in HBMEC where non-target (NT) siRNA had no effect on the expression (B). Data are expressed as mean±SEM from 7 different experiments. *p<0.05 vs control, †p<0.05 vs TNF-α (10 ng/mL), #p<0.05 vs PKC-α + TNF-α.

Figure 5 – 2 columns

PKC-α gene knockdown attenuates the protein expression of all PPS components as well as MMP-2 activity. HBMECs transfected with non-target (NT) siRNA or PKC-α siRNA were cultured in the absence or presence of TNF-α (10 ng/mL) for 6 h. Silencing of PKC-α alone in HBMEC significantly attenuated the effects of TNF-α on all PPS proteins as evidenced by Western analyses (A-D). Transfection with PKC-α siRNA also diminished the levels of intracellular and extracellular MMP-2 activities as shown by gelatin zymograghy (E, F). Data are expressed as mean±SEM from 10 different experiments. *p<0.05 vs NT control, †p<0.05 vs NT + TNF-α (10 ng/mL).

Figure 6 – 1 column

TNF-α reduced the protein expressions of tight junction proteins. HBMEC transfected with non-target (NT) siRNA or PKC-α siRNA were cultured in the absence or presence of TNF-α (10 ng/mL) for 6 h. Treatments with TNF-α decreased both claudin-5 and occludin protein levels. Knockdown of PKC-α gene alone via specific siRNA negated the effects of TNF-α (A, B). Data are expressed as mean±SEM from 6 different experiments. *p<0.05 vs NT control, †p<0.05 vs NT + TNF-α (10 ng/mL).

Figure 7 – 2 columns

TNF-α increased apoptosis, caspase-3/7 activities and cytoskeletal reorganisation. HBMEC transfected with non-target (NT) siRNA or PKC-α siRNA were cultured in the absence or presence of TNF-α (10 ng/mL) for 6 h. Silencing of PKC-α gene alone in endothelial cells attenuated the effects of TNF-α on apoptosis (A, C), caspase-3/7 activities (B) and on actin cytoskeleton (D). Arrows in C and D indicate the TUNEL-positive cells and F-actin stress

fibres. Scale bars = 20μm. Data are expressed as mean±SEM from 6 different experiments. [*]p<0.05 vs NT control, [†]p<0.05 vs NT TNF-α (10 ng/mL), [#]p<0.05 vs siRNA control cells.

Figure 8 – 1 column

PKC-α knockdown attenuated the deleterious effects of TNF-α on BBB integrity and function. HBMEC-HA co-cultures established using endothelial cells transfected with non-target (NT) siRNA or PKC-α siRNA were exposed to TNF-α (10 ng/mL) for 6 h. Silencing of PKC-α gene alone significantly attenuated the effects of TNF-α on TEER (A) and the flux of NaF (B) or EBA (C). Data are expressed as mean±SEM from 6 different experiments. [*]p<0.05 vs NT control, [†]p<0.05 vs NT + TNF-α (10 ng/mL), [#]p<0.05 vs PKC-α siRNA control.

Figure 1

26

Figure 2

A

B

C

Figure 3

A

Pro-MMP-2   72kDa

B

Pro-MMP-2   72kDa

C
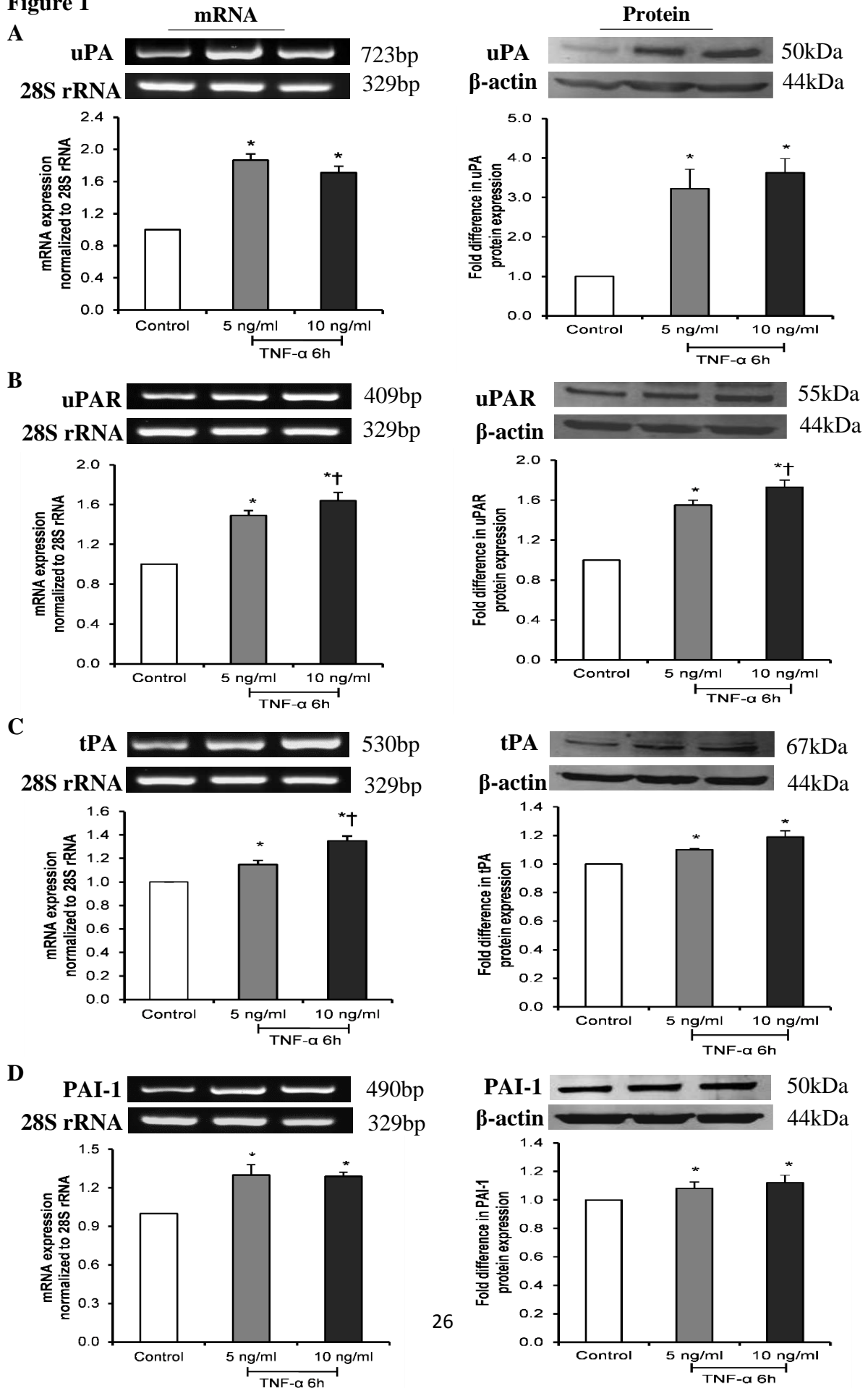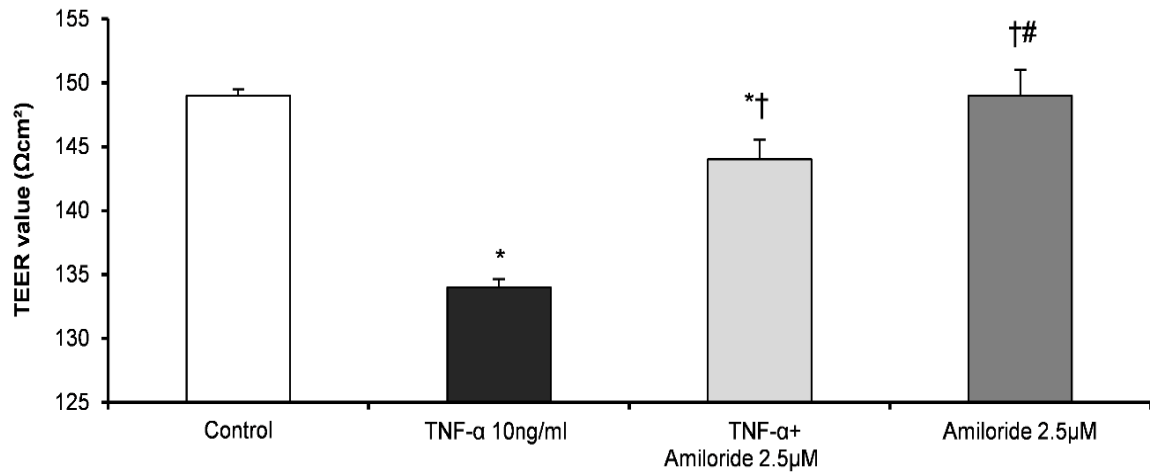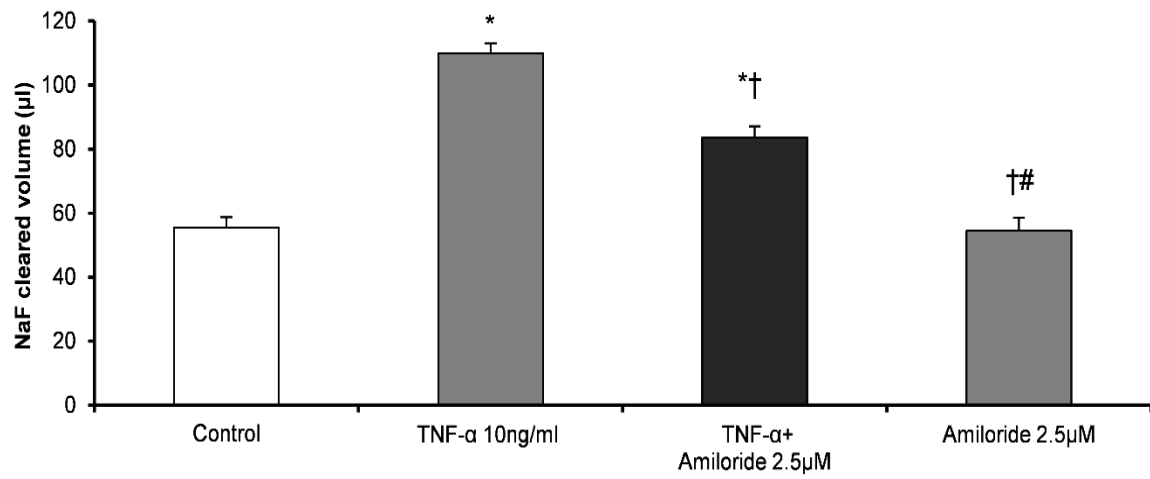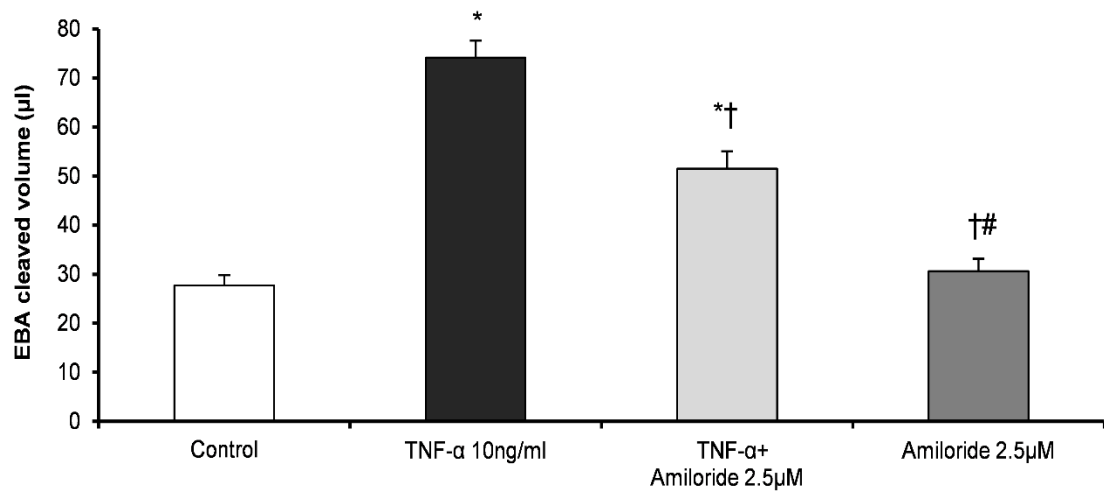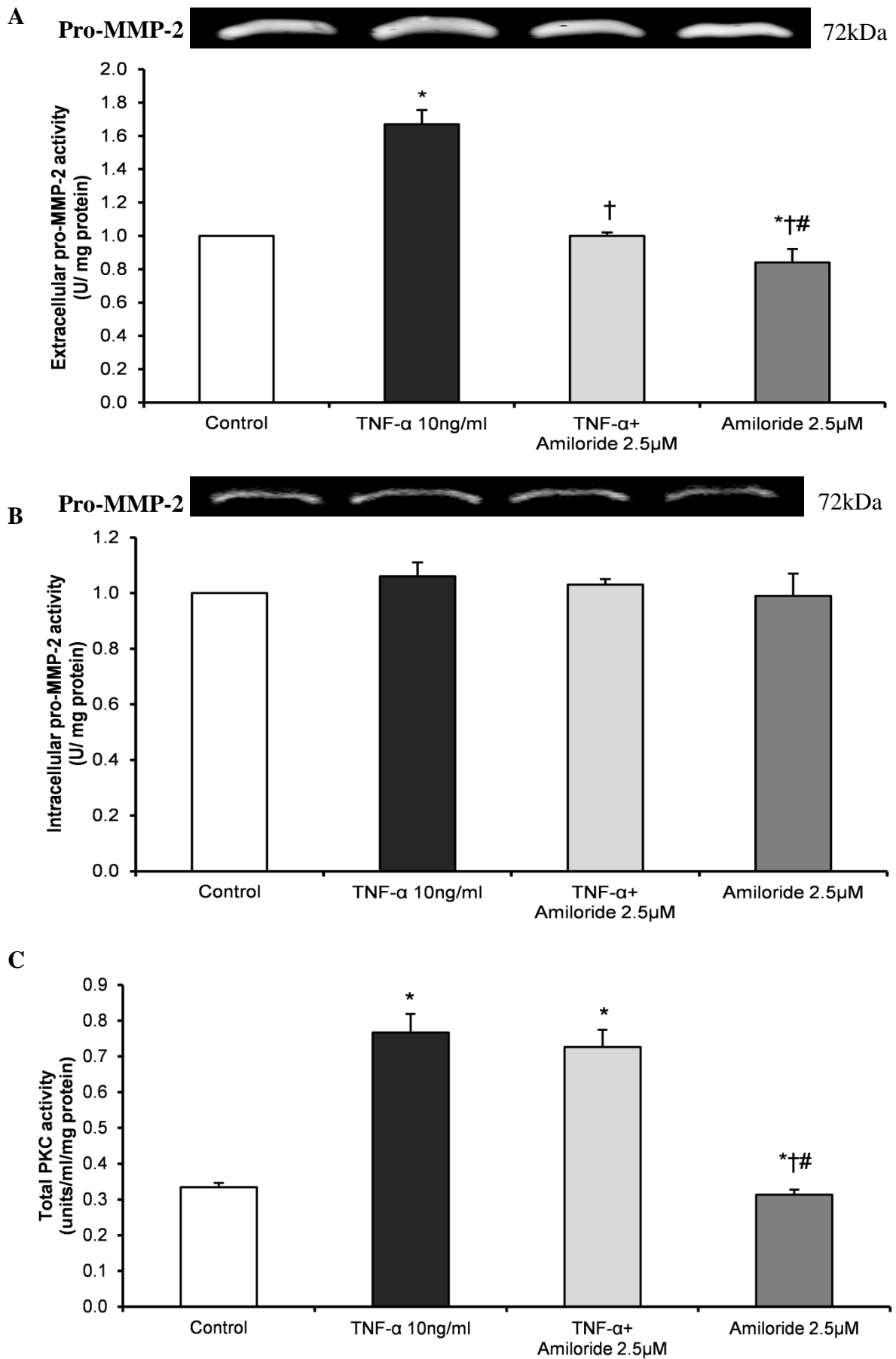
Figure 4

A

B

Figure 5

A

B

C

D

E

F

30

Figure 6

A   Claudin-5

B   Occludin

Figure 7

A

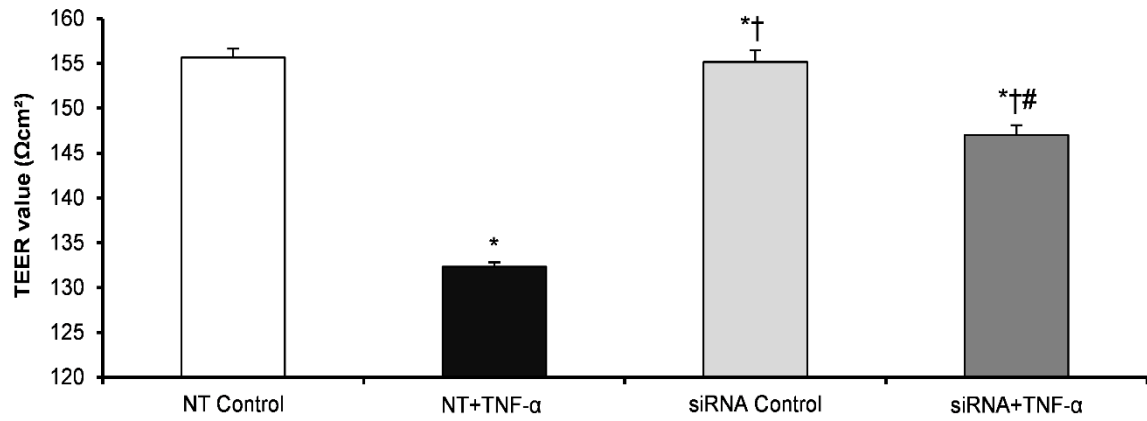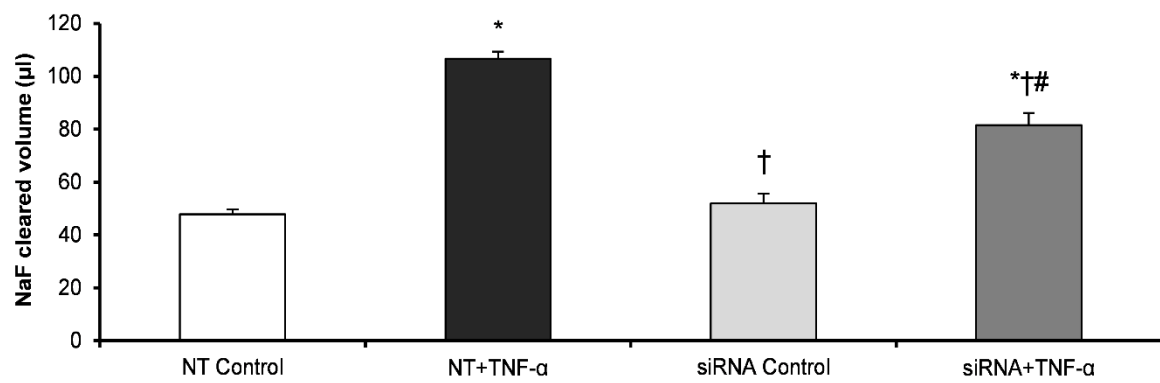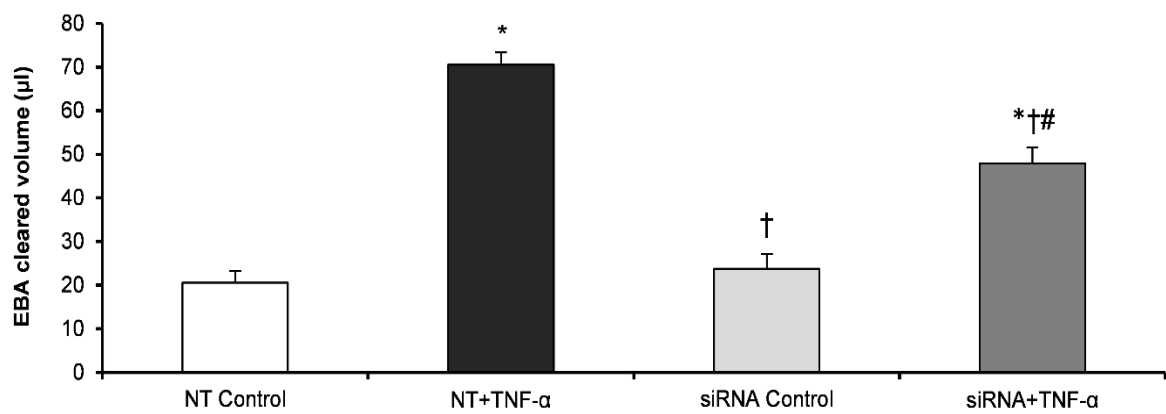

B

C

D
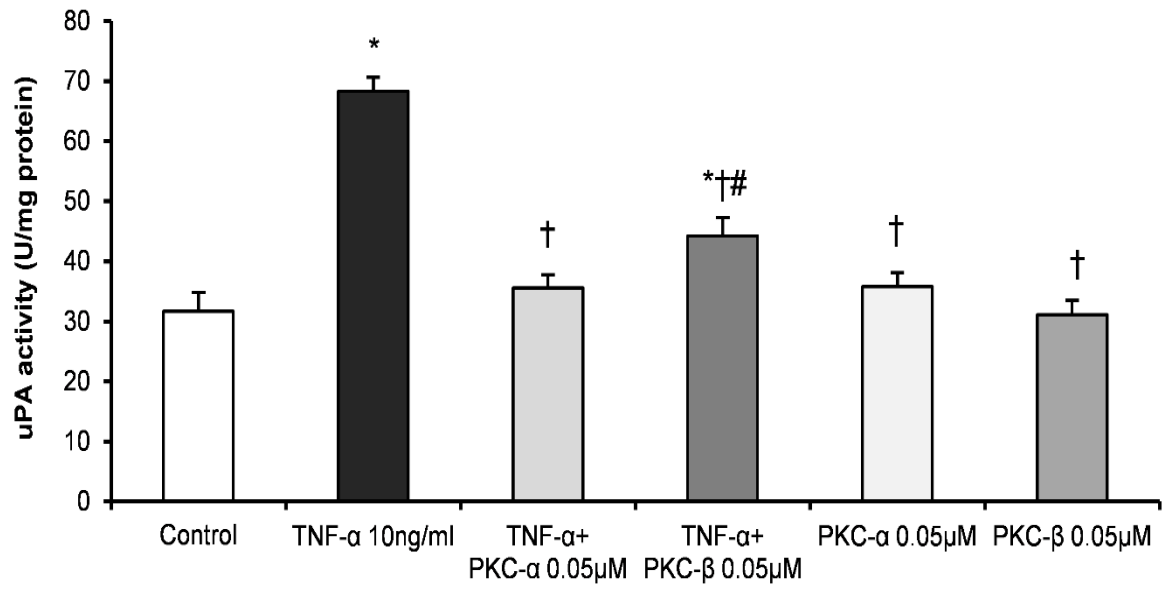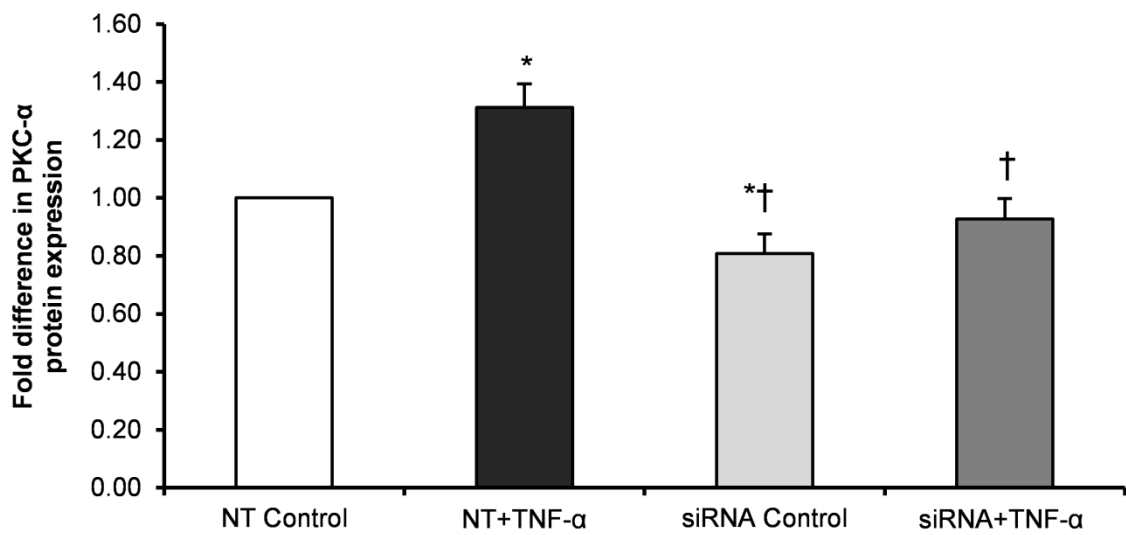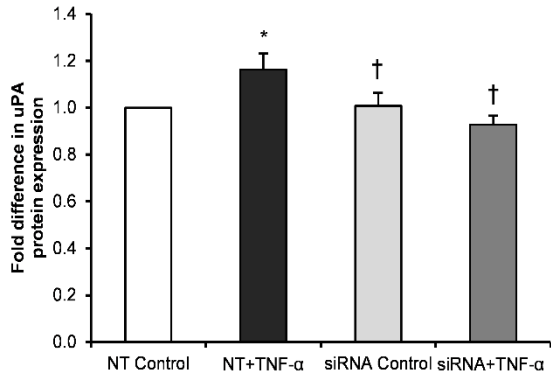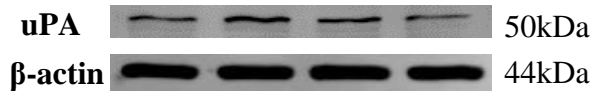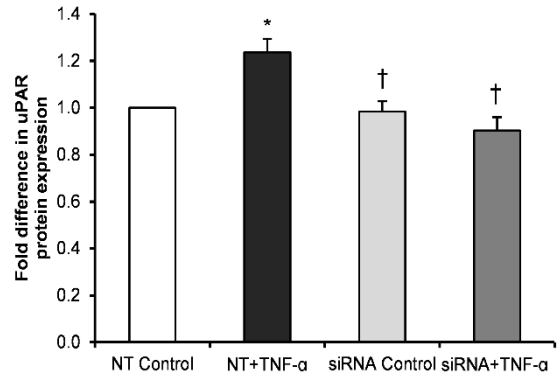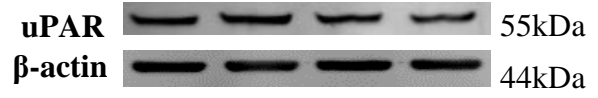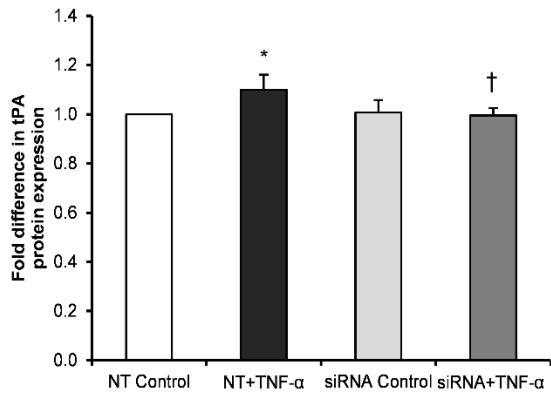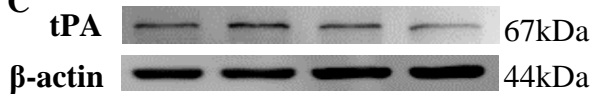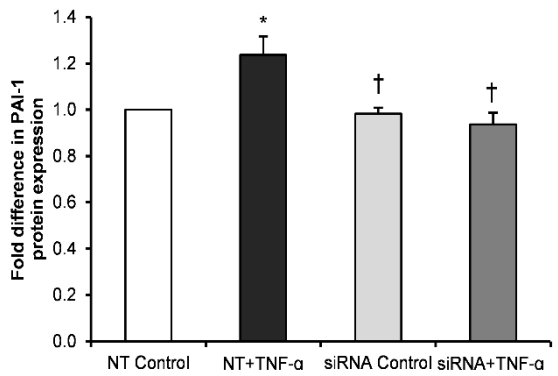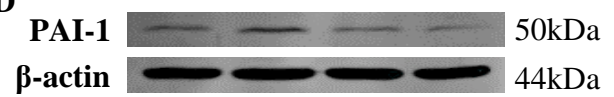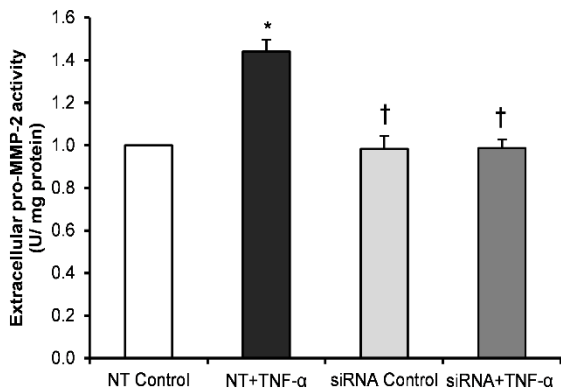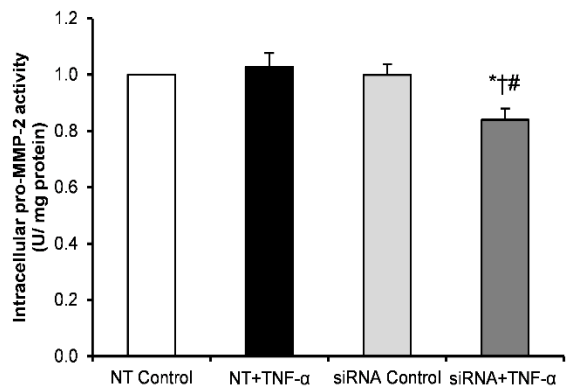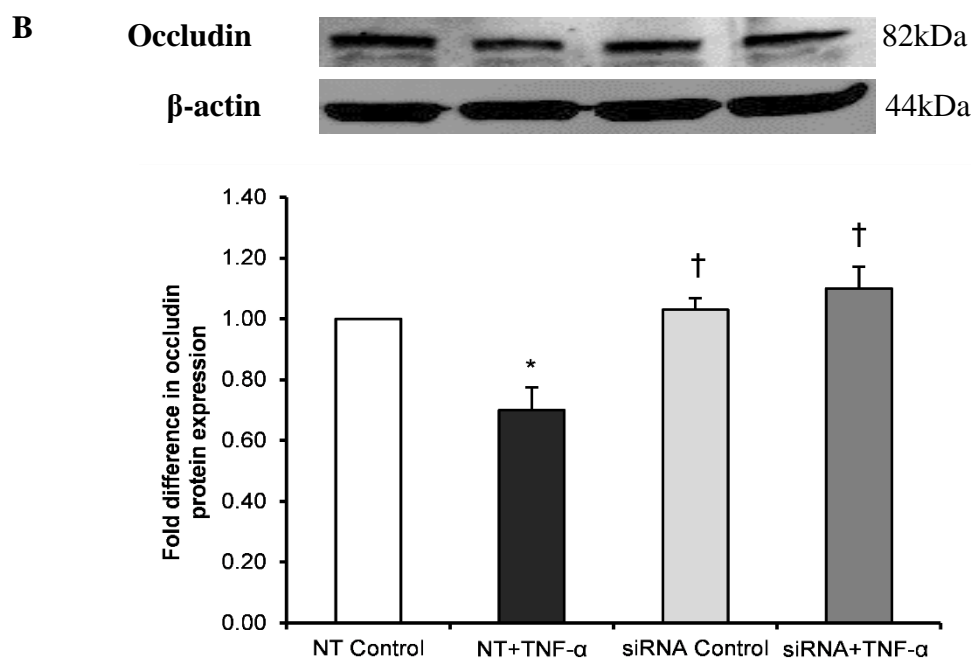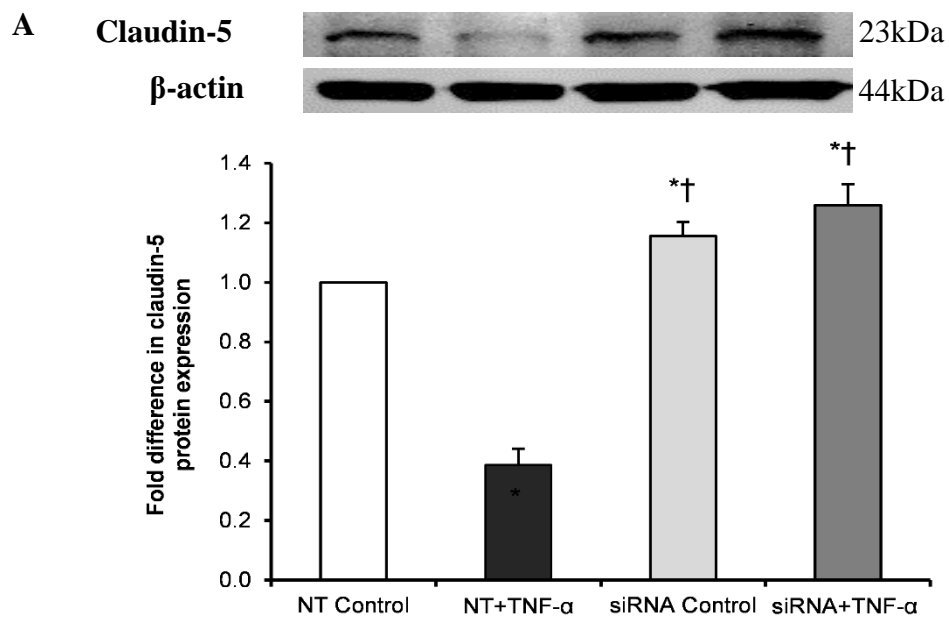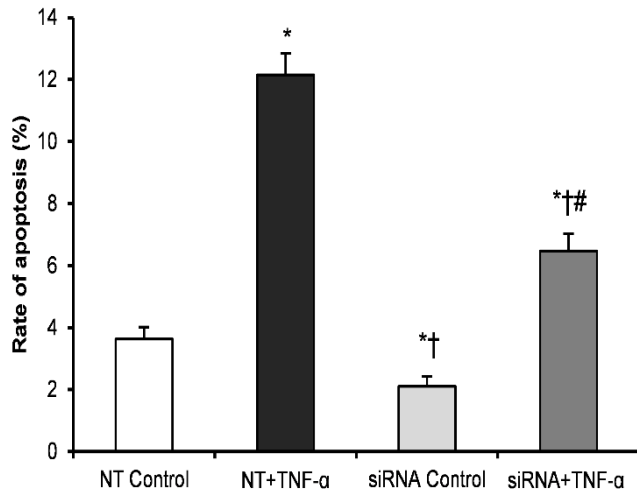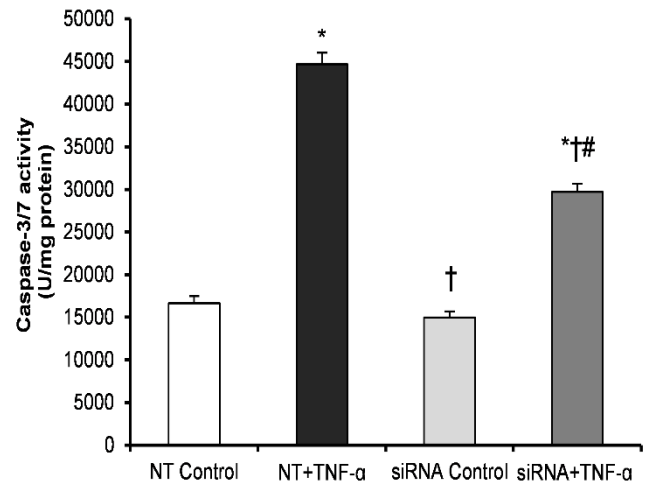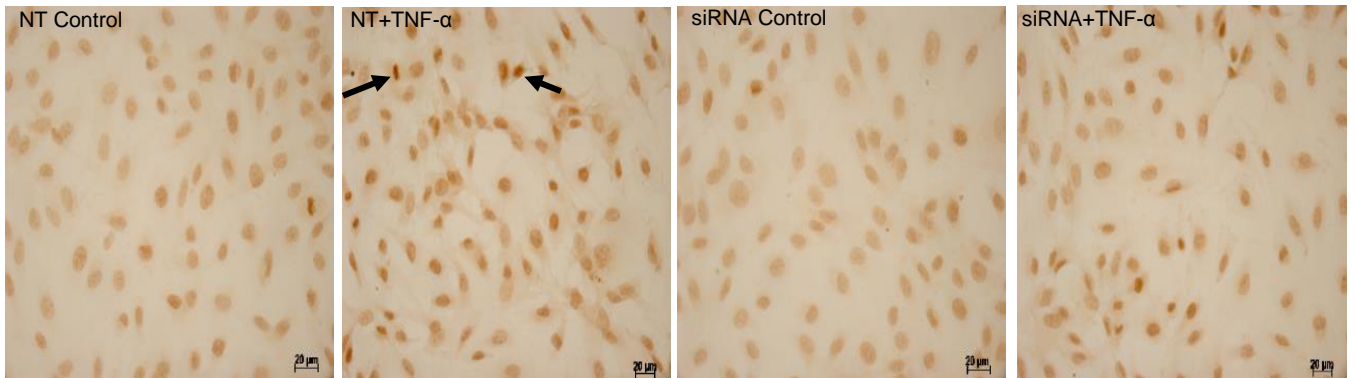
D
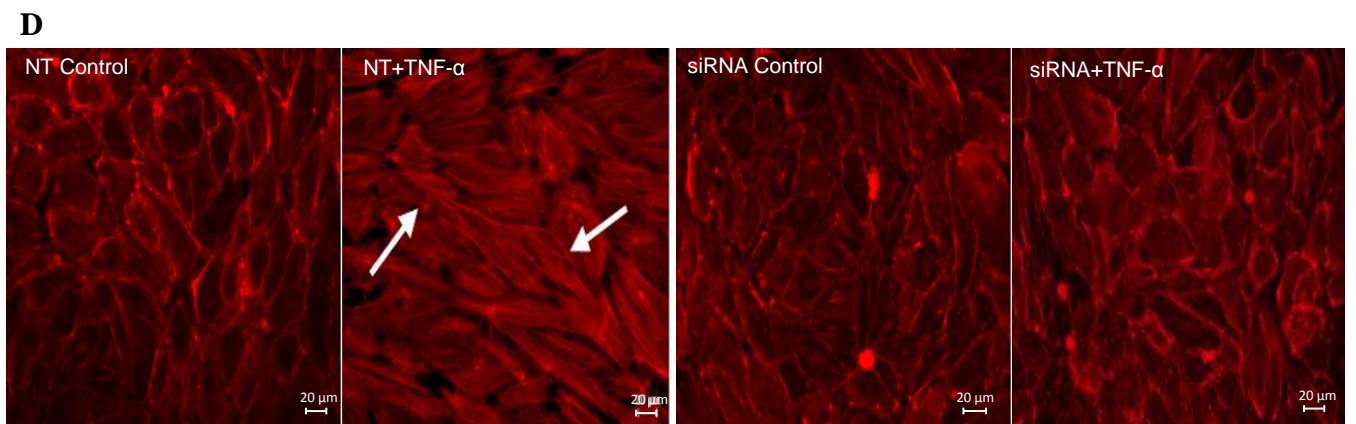
Figure 8

A

B

C

TABLE 1.   Forward and reverse primers used in RT-PCR

PPS component	Forward primer (5' to 3')	Reverse primer (5' to 3')
uPA	TAGGCTCTGCACAGATGGAT	GTGAGGATTGGATGAACTAGGC
tPA	GACGCTGTGAAGCAATCATGGA	CTGGGTTTCTGCAGTAGTTGTG
uPAR	GATCCAGGAAGGTGAAGAAGG	GCAGGAGACATCAATGTGGTT
PAI-1	GTCACATTGCCATCACTCTTGT	GGACTTCCTGAGATACGGTGAC
28S RNA	AAACTCTGGTGGAGGTCCGTAGCGGTCCTG	GCCAGTTCTGCTTACCAAAAGTGGCCAACT

Data are expressed as mean ± SEM (n=9). *$P< 0.05$.